Mat Res Innovat (2001) 5:87–93

ORIGINAL ARTICLE

Y. C. Zhou · X. H. Wang

Deformation of polycrystalline Ti_2AlC under compression

Received: 15 January 2001 / Reviewed and accepted: 12 April 2001

Abstract Deformation of polycrystalline Ti_2AlC under room and high temperature compression was investigated. The results demonstrated that Ti_2AlC was damage tolerant at room temperature and the samples were shear fractured upon failure. At high temperatures Ti_2AlC deform plastically. The brittle-to-ductile-transition temperature (BDTT) of Ti_2AlC was between 1000 °C and 1050 °C. The microstructure and fracture surfaces were examined using scanning electron microscopy. Due to insufficient number of dislocation systems, the room-temperature deformation was constitute of kinking and delaminating of laminated Ti_2AlC grains, basal plane dislocation slip, formation of voids and cavities in the vicinity of main crack. At high temperatures below BDTT, the deformation was a combination of cavities formation and intergranular sliding. At temperatures above BDTT, the deformation was mainly plastic flow.

Keywords Ti_2AlC · deformation · fracture mode · damage mechanism

Introduction

Recent works demonstrated that the layered ternaries like Ti_3SiC_2, Ti_3AlC_2 Ti_2AlC and Ti_2AlN exhibited a unique combination of properties, which are the merits of both metals and ceramics. Generally, these materials are damage tolerant or not-so-brittle at room temperature, electrical conductive, readily machinable and resistant to thermal shock. They also have low density, high strength and modulus, and excellent high-temperature-oxidation resistance. Ti_2AlC is one of the promising layered ternary carbides from this family. Interest in Ti_2AlC emanates from the opportunity provided to tailor properties, since two distinct structurally related ternary phases Ti_2AlC and Ti_3AlC_2 are available in the Ti-Al-C system. Furthermore, the density of Ti_2AlC is lower (4.11 g/cm^3), which is attractive when it is used as a structural material or as reinforcement for polymers and metals.

The structure of Ti_2AlC was deciphered in 1963 by Jeitschko et al [1]. It crystallizes in the Cr_2AlC-type structure with the space group of $P6_3/mmc$. The atoms are located at the following Wyckoff positions: Ti at 4*f*, Al at 2*c* and C at 2*a*. The lattice constants are a=3.04 Å and c=13.60 Å with two formulae per unit cell. Fig. 1 shows the crystal structure of Ti_2AlC. Recent work [2] demonstrated that the properties of Ti_2AlC are strongly related to its crystal and electronic structure. The *ab*

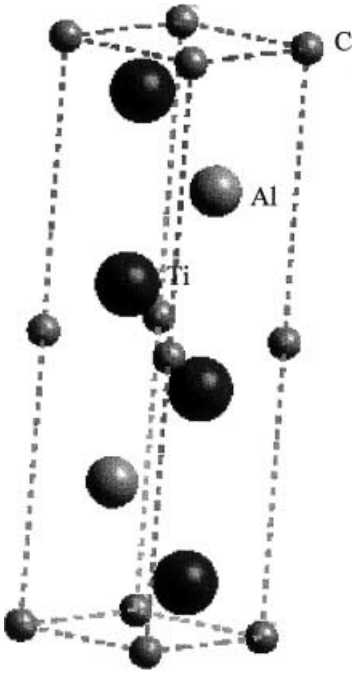

Fig. 1 Crystal structure of Ti_2AlC

Y. C. Zhou (✉) · X. H. Wang
Ceramic and Composite Department, Institute of Metal Research,
Chinese Academy of Sciences, 72 Wenhua Road,
Shenyang 110016, P. R. China
e-mail: yczhou@imr.ac.cn
Tel.: +86-24-23843531, Fax: +86-24-23891320

initio calculations [2] indicated that all three types of bond: metallic, covalent and ionic, had contributions to the bonding in Ti_2AlC. The good electrical conductivity came from the metallic bonding and the high strength and modulus were attributed to the strong Ti-C covalent bond in the structure.

Although Ti_2AlC has salient properties and is promising in use at high temperatures, method for the fabrication of phase-pure Ti_2AlC has not been established. Most of papers concerning Ti_2AlC that can be found in literature described the strengthening effect of Ti_2AlC in TiAl/Ti_2AlC composite [3, 4]. Barsoum et al [5] prepared bulk Ti_2AlC by reactive hot pressing of Ti, Al_4C_3 and graphite powders at 1600 °C for 4 hours. The hardness and the electrical conductivity of the material prepared using this method were 5.5 GPa and 2.8×10^6 $\Omega^{-1}m^{-1}$, respectively. They [6] also fabricated polycrystalline Ti_2AlC by hot isostatic pressing of Ti, Al_4C_3 and graphite powders at 1300 °C for 30 hours. The hardness and electrical conductivity were 4.5 GPa and 2.7×10^6 $\Omega^{-1}m^{-1}$, respectively. The room temperature compressive strength was 540 MPa and the yield point between 1000 °C and 1300 °C were in the range of 270–435 MPa. In both of the samples fabricated by Barsoum et al [5, 6], second phase inclusions of Al_2O_3 were observed. Recently, Wang and Zhou [7] developed a novel solid-liquid reaction synthesis and simultaneous densification method to prepare polycrystalline Ti_2AlC. The method demonstrated the advantages of low synthesis temperature, short reaction time, and simultaneous synthesis and densification. The material prepared by this method was phase-pure Ti_2AlC with the heterogeneous microstructure. The Vickers hardness and electrical conductivity were 2.8 GPa and 4.4×10^6 $\Omega^{-1}m^{-1}$, respectively. And the flexural strength and fracture toughness was 275 MPa and 6.5 $MPa.m^{1/2}$. In the indentation tests [6, 7], no cracks were observed at the corner of the indent and the indentation damage is confined to the immediate vicinity of the indent. This phenomenon is quite analogous to that observed in Ti_3SiC_2 where a number of energy-absorbing mechanisms including diffuse micro cracking, delaminating, crack deflection, grain push-out, and grain buckling contribute to its 'ductility'. Although micro scale ductility and damage of Ti_2AlC were studied in indentation tests, the deformation mechanisms of Ti_2AlC at room and high temperatures were not fully understood and are attractive to material scientists. In this work, we investigate the deformation of polycrystalline Ti_2AlC at room and high temperatures under compression. The mechanisms of damage tolerance at room temperature and deformation at elevated temperatures were discussed based on the microstructure and fracture surface analysis.

Relation to the previous work

Although the structure of Ti_2AlC was reported in 1963 [1], there are only a few of papers concerning the preparation or properties of this material. Most of them described the strengthening effect of Ti_2AlC in TiAl [3, 4]. Recent interest in Ti_2AlC was stimulated by the disclosure of the unusual properties in the layered ternary ceramics like Ti_3SiC_2, Ti_3AlC_2, Ti_2AlC and Ti_2SnC [2, 8–12]. Zhou and Sun [2] investigated the electronic structure of Ti_2AlC and demonstrated that all three types of bond: metallic, covalent and ionic, had contribution to the bonding in Ti_2AlC. They explained the properties of Ti_2AlC using the electronic structure and bonding properties. Barsoum et al [5] prepared Ti_2AlC by reactive hot pressing and hot isostatic pressing method [6]. They demonstrated that Ti_2AlC exhibited metallic conductivity [5, 6]. The deformation of Ti_2AlC at room and high temperature (1000–1300 °C) under compression was described [6]. At room temperature the compressive strength of Ti_2AlC was 542 MPa and at high temperatures between 1000–1300 °C the yield points were in the range of 270–435 MPa. Wang and Zhou [7] developed a solid-liquid reaction synthesis and simultaneous densification method for preparing pure Ti_2AlC. But the deformation mechanisms of polycrystalline Ti_2AlC were not discussed in detail in previous works [6, 7]. The main contributions of this work are first give details on the deformation of polycrystalline Ti_2AlC under compression from room temperature to 1200 °C; and then investigated the deformation mechanisms through fractographic analysis and comparison of the microstructure change before and after deformation.

Experimental

The material used in this work is polycrystalline Ti_2AlC, which was fabricated by the solid-liquid reaction and simultaneous densification process utilizing Ti, Al and graphite powders as initial materials. Details of the solid-liquid reaction and simultaneous densification process for the preparation of Ti_2AlC were given elsewhere [7]. In this process, Al melted at 660 °C and then the melting aluminum provides a favorable liquid circumstance for the reactions between aluminum and titanium to form TiAl and Ti_3Al at temperature of ~850 °C. At higher temperatures, TiC formed and reacted with TiAl at ~1100 °C to yield the layered ternary compound Ti_2AlC. Briefly, the preparation procedure is as follows. Ti, Al and graphite powders were mixed and milled in a polypropylene jar for 10 hours. After ball milling, the mixed powders were cold pressed into a disc of 50 mm in diameter and then put in a graphite die. The solid-liquid reaction and simultaneous densification of Ti_2AlC was conducted under a flowing Ar atmosphere in a furnace using graphite as heating element. The hot pressing temperature was 1400 °C and the applied pressure was 30 MPa. The bulk density of the polycrystalline Ti_2AlC was 4.10 g/cm^3, which is near the theoretical density of Ti_2AlC.

Samples for the compressive testing were cylinders of 5.0 mm in diameter and 8.0 mm in height. The compressive test specimen were electrical-discharge machined from the bulk material. The compressive tests were performed on a Gleeble-1500 universal-testing machine (Gleeble Inc., USA) at a strain rate of 1×10^{-4} s^{-1}. The fracture surfaces and microstructure change of the samples before and after high temperature compression were examined in an s-360 scanning electron microscope (Cambridge Instruments, UK).

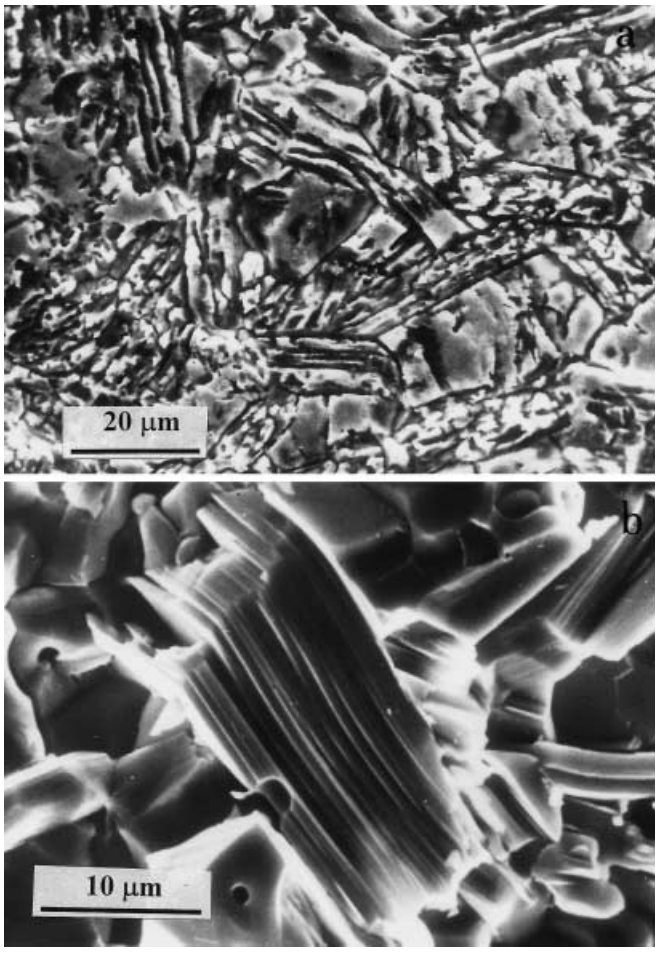

Fig. 2 **a** Microstructure of polycrystalline Ti_2AlC, a heterogeneous microstructure is shown. **b** SEM micrograph of fracture surface, the anisotropic and layered nature of the material are revealed

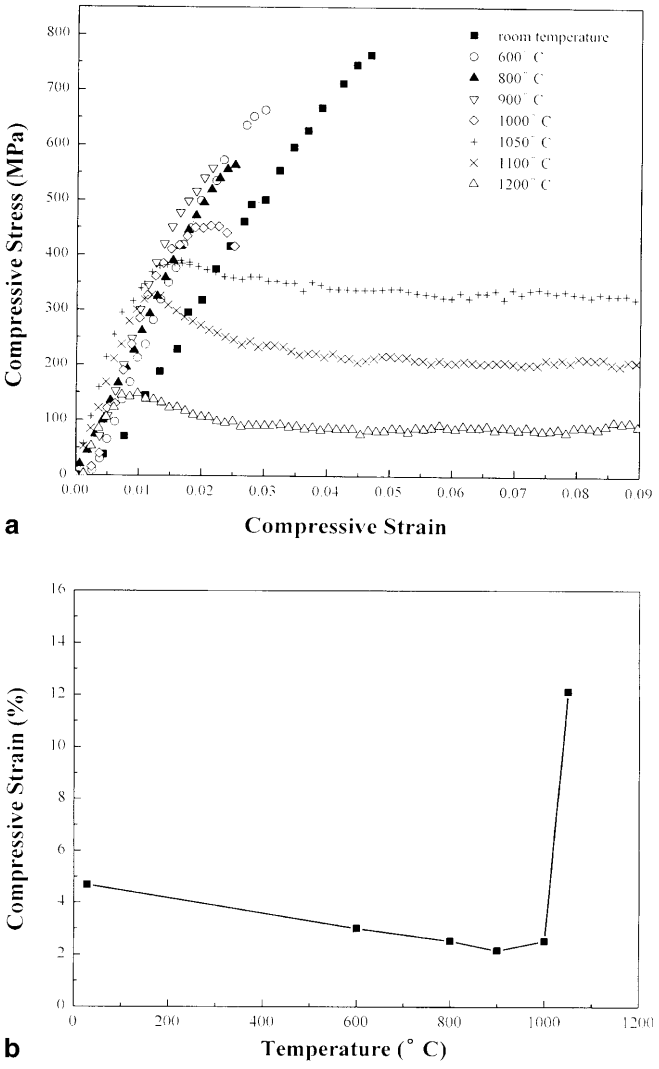

Fig. 3 **a** Compressive stress-strain curves of polycrystalline Ti_2AlC tested at room temperature and high temperatures up to 1200 °C. **b** The compressive strain of polycrystalline Ti_2AlC as a function of testing temperature

Results

X-ray diffraction analysis revealed that the material fabricated by the solid-liquid reaction and simultaneous densification process using stoichiometric mixture of Ti, Al, and graphite powders as initial materials composed of only Ti_2AlC. No impurity phase in crystalline form was identified. The bulk density measured by Archimedes method was 4.10 g/cm^3, which is near the theoretical density of Ti_2AlC (4.11 g/cm^3). The microstructure investigation demonstrated a heterogeneous microstructure feature of this material, i.e. large size laminated grains were embedded in equiaxial grains, which is analogous to that of platelets reinforced ceramic matrix composites [13]. Fig. 2 (a) shows a SEM micrograph of the polished surface after etching with HNO_3+HF+H_2O solution. Evidence of full densification is seen from the figure. The laminated Ti_2AlC grains are 5–10 μm in thickness and are composed of a number of micro-laminate. Fig. 2 (b) shows a SEM micrograph of the fracture surface of polycrystalline Ti_2AlC, in which the anisotropic and layered nature of this material is revealed.

The compressive stress-strain curves of polycrystalline Ti_2AlC tested at different temperatures are shown in Fig. 3 (a). The temperature range was from room temperature to 1200 °C and the strain rate was 1×10^{-4} s^{-1}. It is seen from the figure that the room-temperature compressive stress-strain curve derived from linearity. In fact, the sample underwent a number of loading-relaxation-reloading processes before failure. The maximum stress and the pseudo-plastic deformation strain upon failure for polycrystalline Ti_2AlC was 763 MPa and 4.8%, respectively. After reaching the maximum strength, the sample still remained its integrity, i.e. it did not separated into two parts. This phenomenon indicates that Ti_2AlC is a not-so-brittle material. With the increase of testing temperature, the stress upon failure decreased. At temperatures above 1050 °C, the material deformed plastically. At 1100 °C, the cylinder sample of 8.0 mm in height can be compressed into a flat pancake of ~5 mm

in height without failure. Fig. 3 (b) shows the dependence of compressive strain on testing temperature wherein a sharp increase in the plastic strain is seen at 1000–1050 °C. Because of the abrupt increase in the plasticity between 1000 °C and 1050 °C, we assume this temperature range is the brittle-to-ductile-transition temperature (BDTT) for polycrystalline Ti_2AlC.

One trait that can be seen in Fig. 3 (b) is that the compressive strain decreased with the increasing temperature in the temperature range of RT to 900 °C and then increased with the testing temperature above 900 °C. Careful analysis of the compressive stress-strain curves shown in Fig. 3 (a), we can also find the similar change in the linear part of the stress-strain trajectory. The slop in the linear part of the stress-strain trajectory increased with the temperature below 1050 °C and decreased with the temperature above 1050 °C. The maximum slop in the linear part of the compressive stress-strain curve is observed at 1050 °C. This phenomenon is analogous to the flow stress anomaly in Ti_3SiC_2 reported by Sun et al [14], wherein a maximum peak of yield stress was observed at 950 °C. In this work, the plot of yield stress versus temperature was not given due to the difficulty in determining the yield point accurately from the stress-strain curves in Fig. 3 (a). But strain versus temperature curve and the change of the slop in the linear part of stress-strain trajectories indicate that Ti_2AlC is stronger at 900 °C. Stress anomaly was observed in a number of polycrystalline and single-crystal intermetallics [15–18] but seldom observed in ceramic material [14]. The mechanisms for anomalous flow of layered carbides like Ti_3SiC_2 and Ti_2AlC are not known. We will discuss this in later sections.

To understand the deformation mechanism and fracture mode of polycrystalline Ti_2AlC, the samples after compressive testing were examined in scanning electron microscopy. Fig. 4 (a) shows a SEM micrograph of the surface of a cylinder sample after loading to a maximum stress of 763 MPa at room temperature. The left part of the figure is a low magnification micrograph of the sample surface and the right part is a large magnification micrograph of the rectangular area of the left part. It is seen from the figure that the main crack propagated along ~45° off the axis of the cylinder, namely loading direction. It is also seen that the damage was confined to the vicinity of the crack. Evidences of the formation of voids and cavities, branching and deflecting of the main cracks, pull-out of the Ti_2AlC grains and bridging of two halves of the sample by laminated Ti_2AlC grains are clearly seen in the right part of the figure. The SEM observation demonstrated that Ti_2AlC was shear fractured at room temperature and the damage was confined through formation of voids and cavities, branching and deflecting of the main cracks, and pull-out of the Ti_2AlC grains. Fig. 4 (b) is a SEM micrograph of the fracture surface of a manually separated part of the sample after compression in which micro-scale deformation of polycrystalline Ti_2AlC is shown. Kinking and delaminating of Ti_2AlC grains are obvious in the figure. Break-up of

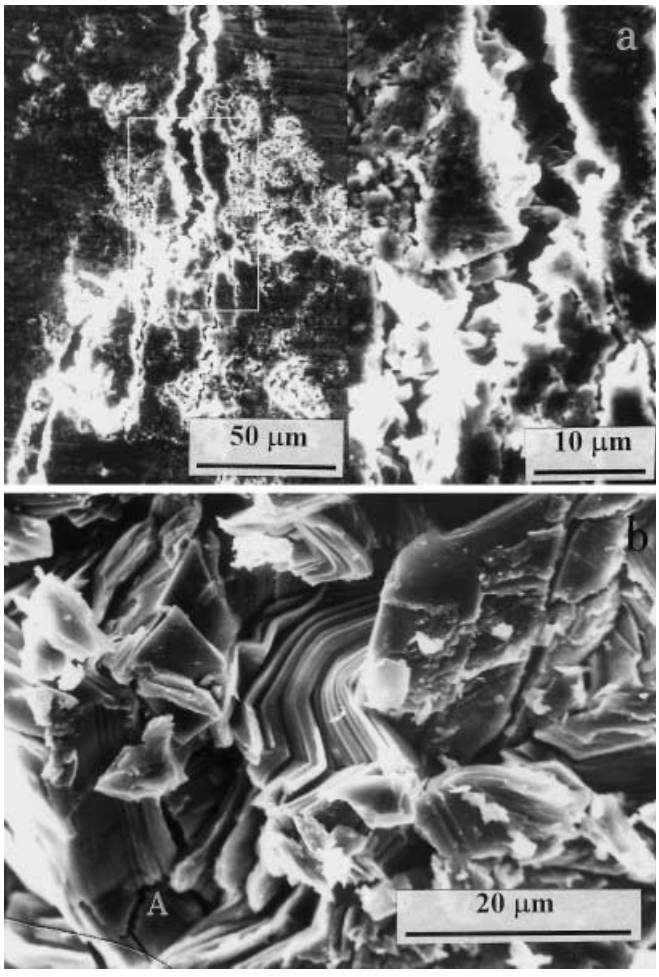

Fig. 4 **a** Microstructure of a sample surface after room temperature compressive test. **b** SEM micrograph of the fracture surface of the sample shown in **a** micro-scale deformation due to kinking and delaminating of laminated Ti_2AlC grains is shown

the laminated grains can also be seen in Fig. 4 (b), as marked A in the figure. However, delaminating crack was confined within the laminated Ti_2AlC grains indicating that Ti_2AlC had the ability to confine the damage. Kinking and delaminating were observed in deformed Ti_3SiC_2 [19, 20] and their contribution to the damage confinement of Ti_3SiC_2 were discussed in previous papers. In Ti_2AlC, our SEM observations revealed that kinking, delaminating and pull-out of Ti_2AlC grains, formation of cavities and crack branching are the main contributions to the room temperature deformation and damage confinement of polycrystalline Ti_2AlC.

When the testing temperature increased, the samples still shear fractured below 1000 °C. Fig. 5 (a) shows a SEM micrograph of the surface of a sample after compressive testing at 1000 °C. The sample was shear fractured and maintained the integrity after testing. Careful analysis of the main crack and the enlarge part of the figure, it is interesting to note that the portion that linked the two sides of the crack or shear band increased compared to the specimen tested at room temperature. To

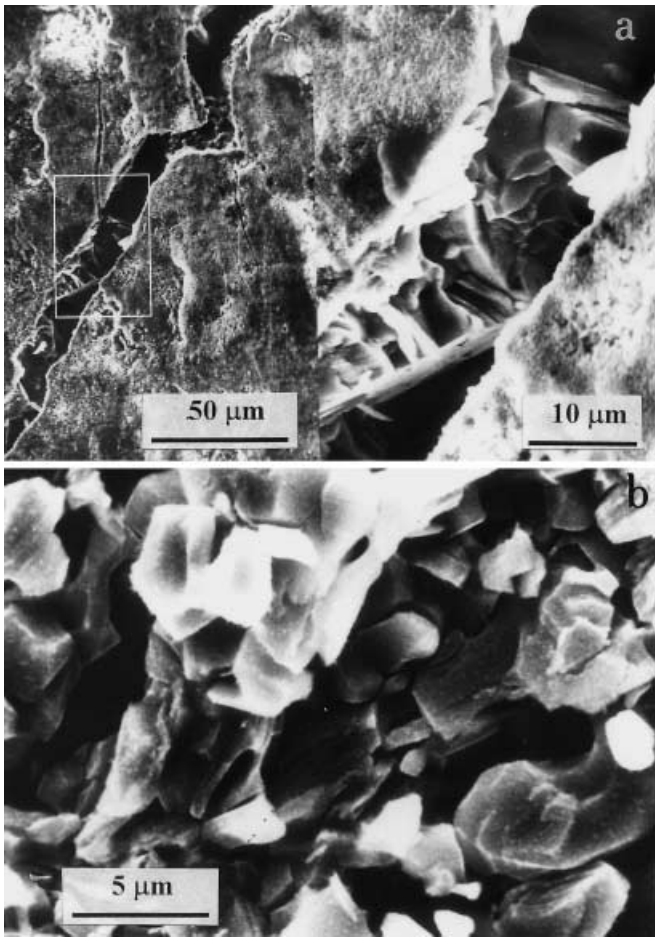

Fig. 5 **a** Microstructure of a sample surface after compression at 1000 °C. **b** Fracture surface of the sample shown in (**a**).

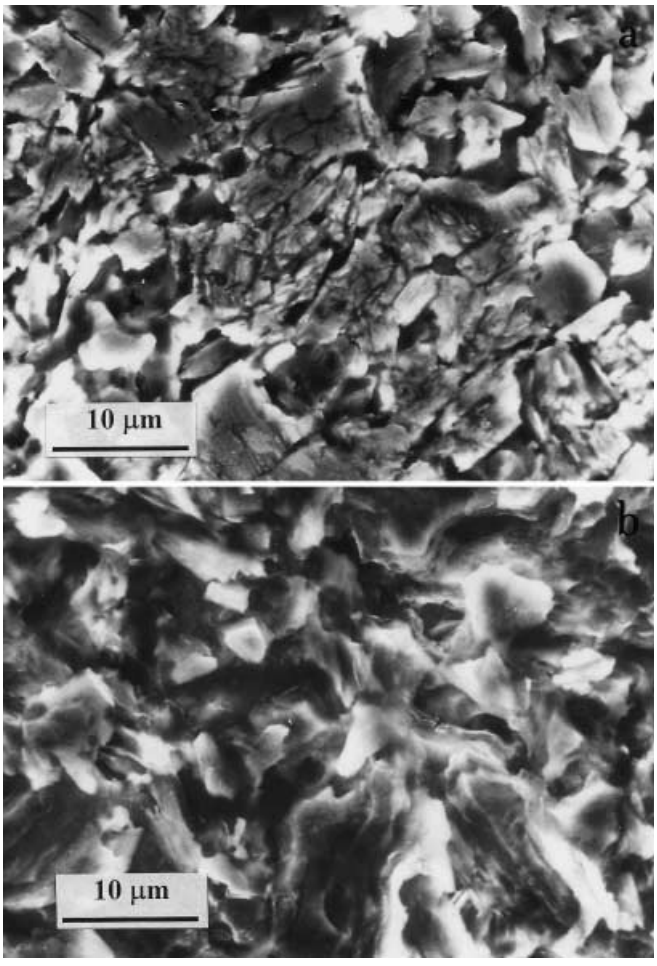

Fig. 6 **a** Microstructure of a sample deformed at 1050 °C. **b** Microstructure of a sample deformed at 1100 °C

further understand the fracture behavior, the sample shown in Fig. 5 (a) was separated and the fracture surface was examined. Fig. 5 (b) shows the fracture surface of the sample after compressive testing at 1000 °C. The main trait of the figure is that the layered nature of the material was not revealed. Cavities and transgranular cracks were seen on the fracture surface. Compared to the SEM micrograph shown in Fig. 2 (a), we noticed that the grain size was significantly reduced in the sample after 1000 °C compressive testing.

The samples tested at temperatures above 1050 °C were plastically deformed and were not fractured after compressed into a pancake. To compare the microstructure change and to understand the deformation mechanism, the compressive deformed specimens were cut in the half height of the pancake, and then polished, etched and observed in scanning electron microscopy. Fig. 6 (a) and (b) show the etched surface of the specimens deformed at 1050 °C and 1100 °C, respectively. In the 1050 °C deformed sample (Fig. 6 (a)), cavities and transgranular cracks are clearly seen. Trace for the rotating of the Ti_2AlC grains can also be seen in the figure. The grain size was reduced compared to the microstructure of the as-prepared material shown in Fig. 2 (a). The large laminated grains were broken up into small pieces and the layered nature of Ti_2AlC could not be seen. In the sample deformed at 1100 °C, evidence of plastic flow of the material is clearly shown in Fig. 6 (b).

Discussion

The experimental results allow an investigation into the deformation mechanisms of Ti_2AlC under compression at both room and high temperatures. They will be discussed in the following sections.

Deformation of Ti_2AlC under room temperature compression:

The microstructure investigation revealed that polycrystalline Ti_2AlC had a heterogeneous microstructure. The large laminated Ti_2AlC grains were distributed within small equiaxial grains. Careful analysis of the SEM micrographs shown in Fig. 2, it is found that the laminated

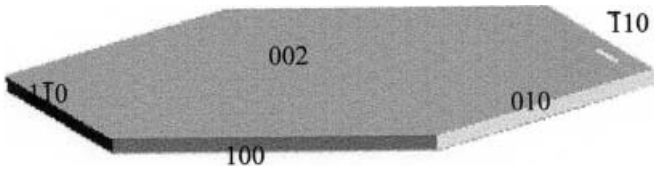

Fig. 7 Computer simulated crystallite shape of Ti_2AlC

grains consisted of a number of hexagonal thin slices or micro-lamella. The hexagonal slice or micro-lamella is the typical crystallite shape of the layered ternary compound of Ti_3SiC_2 [21] and Ti_2AlC which crystallize in hexagonal structure. Computer simulated crystallite shape (Fig. 7) using the *Morphology* code in Cerius^2 computational program for material research based on the Donnay-Harker [22, 23] theory shows that the hexagonal surfaces in Fig. 7 are parallel to {002} and the side surfaces are parallel to {100} planes of Ti_2AlC. The thin hexagonal slices or micro-lamellae constitute the laminated Ti_2AlC grains. The formation of the hexagonal slices in Ti_3SiC_2 was discussed in the earlier work [21]. According to the Donnay-Harker theory, they are formed when the growth rate on {002} is the slowest among that of {002}, {100} and {101} surfaces. In Ti_3SiC_2 the hexagonal slices are weakly bonded [24] allowing easy shear slip. The weak boundaries between the thin lamellae may also act to suppress macro-fracture by deflecting incipient surface cracks away from the directional tensile stress trajectory [24] making it not sensitive to damage. In Ti_2AlC, delaminating and shear slip of the laminated grains are also observed in the indentation tests [7]. The easy shear slip and delaminating of Ti_2AlC hexagonal slices suggested that they be also weakly bonded. The easy shear slip and the ability to confine the damage within the weakly bonded micro-laminate making polycrystalline Ti_2AlC is damage tolerant.

The investigation on the room temperature compressive properties of Ti_2AlC demonstrated that the stress-strain curve derived from linearity and the sample underwent a number of loading-relaxation-reloading processes before failure (Fig. 3 (a)). SEM observation (Fig. 4 (a)) of the sample after compression test revealed that the sample was shear fractured and the damage was confined to the vicinity of the main crack or shear band through the formation of voids and cavities, deflecting and branching of the main crack, delaminating and pull-out of laminated Ti_2AlC grains. Thus the loading-relaxation-reloading processes in the stress-strain curve were caused due to the formation and confinement of damages within the material during the loading procedure. In fracture surface analysis, micro-scale plastic deformation (Fig. 4 (b)) was observed in polycrystalline Ti_2AlC, which is quite similar to the phenomenon observed in polycrystalline Ti_3SiC_2 [19, 20]. It is seen from Fig. 4 (b) that kinking and delaminating of laminated Ti_2AlC grains, together with the intergranular fracture are the main deformation mode of polycrystalline Ti_2AlC under compression. Barsoum et al [20] proposed that the deformation mode for Ti_3SiC_2 was shear band formation by dislocation arrays, cavitations, creation of dislocation walls and kink boundaries, buckling and delaminating of Ti_3SiC_2 grains. Ti_2AlC has the same space group of $P6_3/mmc$ with Ti_3SiC_2. The structure difference between Ti_2AlC and Ti_3SiC_2 is that in Ti_2AlC every layer of Ti_6C octahedron is separated by a layer of two-dimensional-closed-packed Al atoms, while in Ti_3SiC_2 every two edged-shared layers of Ti_6C octahedra are separated by a layer of two-dimensional-closed-packed Si atoms. At room temperature, only basal plane dislocations are movable in these layered compounds [20]. Slip trace of the basal plane dislocations was observed in Ti_3SiC_2 [25]. Due to the complex crystal structure and insufficient number of slip systems, the deformation modes for polycrystalline Ti_2AlC at room temperature are a combination of delaminating and kink-band formation of the laminated grains, dislocation slip and intergranular fracture.

Deformation of Ti_2AlC at high temperatures:

The stress-strain curves in Fig. 3 (a) demonstrated that the increase in the tested temperature led to gradual decrease of the stress upon failure below 1000 °C. Above 1050 °C polycrystalline Ti_2AlC deform plastically. The compressive strain versus testing temperature (Fig. 3 (b)) shows that the strain upon failure is low at temperatures below 1000 °C and increases dramatically above 1000 °C. Because of the sharp increase in the plasticity between 1000 °C and 1050 °C, we assume this temperature range is the brittle-to-ductile-transition temperature (BDTT) for Ti_2AlC at the strain rate of $1\times10^{-4}s^{-1}$. Beside changes in ductility at different temperatures, the fracture morphology was also changed with the increase of temperature. At room temperature, kinking and delaminating, intergranular shear fracture mode was observed (Fig. 4 (b)); while at 1000 °C the failure is a mixed mode intergranular and transgranular. The fracture morphology of samples tested above 1050 °C can not be obtained since the samples did not failure. The polished and etched surface at half height of the deformed sample revealed the microstructure change before and after deformation. In the sample after deformed at 1050 °C, trace of the rotation of the grains, cavities and transgranular cracks are seen (Fig. 6 (a)). In the sample after deformed at 1100 °C evidence of plastic flow of the material is clearly shown (Fig. 6 (b)). In both of the samples the large laminated grains were broken up into small ones and the layered nature of Ti_2AlC could not be seen. The disappearance of the layered nature in high temperature deformed sample suggested that the bonding between thin hexagonal layers became stronger in polycrystalline Ti_2AlC.

We have known that the low ductility and intergranular fracture at room temperature are due to insufficient number of operative slip system. At high temperatures below BDTT, our SEM observations demonstrate the de-

formation mechanisms are formation of cavities, grain rotation and grain boundary sliding which led to the formation of small grains and transgranular fracture (Fig. 6(a)). Since BDTT is a thermally activated process which is controlled by the mobility of dislocations [26]. Thus the deformation mechanism at temperatures above BDTT was attributed to the availability and mobility of sufficient dislocation systems. Fig. 6 (b) clearly shows the plastic flow of Ti_2AlC grains. But the exact dislocation systems that are available and movable above BDTT are not known now. We must acknowledge that more work on the investigation of dislocation sources in Ti_2AlC is needed in order to understand the high temperature deformation mechanisms of Ti_2AlC.

Knowing the fracture mode is helpful in understanding the strain vs. temperature curve in Fig. 3(b), where a decrease in the strain with the temperature below 900 °C and an increase in the strain with the temperature above 900 °C are shown. In Fig. 3(a) the slop of the linear part of stress-strain trajectory increase below 1050 °C and decrease above 1050 °C with the temperature with a maximum at 1050 °C. This phenomenon is similar to the anomalous flow stress behavior observed in Ti_3SiC_2 [14]. Sun et al [14] tried to explain the anomalous flow stress behavior of Ti_3SiC_2 using the well accepted Kear-Wilsdorf mechanism [27], but found it not applicable since the flow stress of Ti_3SiC_2 was strongly dependent on the strain rate. In this work we explain the phenomenon shown in Fig. 3 using the results of microstructure and fractographic analysis. We know from the microstructure analysis that polycrystalline Ti_2AlC exhibited anisotropic and laminated microstructure feature. The laminated Ti_2AlC grains are composed of a number of thin hexagonal slices. At room temperature the thin hexagonal slices are weakly bonded allowing easy shear slip which contribute to the large compressive strain. In other words, kinking and delaminating, shear slip of the laminated grains, buckling of the Ti_2AlC grains constitute the compressive strain at room temperature. At high temperatures, our SEM observation on the microstructure and fracture surfaces revealed that the bonding between the thin hexagonal slices became stronger thus slip of the hexagonal slices or micro-laminate were inhibited resulting in less contribution to the compressive strain. At temperatures above BDTT, there is sufficient number of movable dislocations and the compressive strain increases significantly.

Conclusion

Polycrystalline Ti_2AlC exhibited anisotropic and layered microstructure. The laminated Ti_2AlC grains composed of a number of thin hexagonal slices, which are weakly bonded and allowing shear-slip. At room temperature, polycrystalline Ti_2AlC was damage tolerant and shear fractured under compression load. Due to insufficient number of dislocation systems, the room-temperature deformation was constitute of kinking and delaminating of laminated Ti_2AlC grains, basal plane dislocation slip, formation of voids and cavities in the vicinity of main crack. At high temperatures Ti_2AlC deform plastically. The brittle-to-ductile-transition temperature (BDTT) of Ti_2AlC was between 1000 °C and 1050 °C. At high temperatures below BDTT, the deformation was a combination of cavities formation, grain rotating and intergranular sliding. At temperatures above BDTT, due to availability and mobility of sufficient number of dislocation systems the deformation was mainly plastic flow.

Acknowledgement This work was supported by the National Outstanding Young Scientist Foundation for Y. Zhou under Grant No. 59925208, the National Science Foundation of China (NSFC) under Grant No. 59772021, 50072034 and '863' program.

References

1. Jeitschko W, Nowotny H, Benesovky F (1963) Monotsch Chem 94:672
2. Zhou YC, Sun ZM (2000) Phys Rev B 61:12570
3. Ramaseshan R, Kakitsuji A, Seshadri SK, Nair NG, Mabuchi H, Tsuda H, Matsui T, Morii K (1999) Intermetallic 7:571
4. Mater SF, Le Petitcorps Y, Etourneau J (1998) Comput Mater Sci 10:314
5. Barsoum MW, Brodkin D, Elraghy T (1997) Scripta Mater 36:535
6. Barsoum MW, Ali M, Elraghy T (2000) Metall Mater Trans A 31:1857
7. Wang XH, Zhou YC (2001) to be published Z Metallkd
8. Zhou YC, Sun ZM, Chen SQ, Zhang Y (1998) Mater Res Innovat 2:142
9. Zhou YC, Sun ZM, Sun JH, Zhang Y, Zhou J (2000) Z Metallkd 91:329
10. Tzenov NV, Barsoum MW (2000) J Am Ceram Soc 83:825
11. Zhou YC, Dong HY, Yu BH (2000) Mater Res Innvat 4:36
12. Zhou YC, Dong HY, Wang XH, Chen SQ (2000) J Phys: Condensed Mater 12:9617
13. Chou YS, Green DJ (1993) J Am Ceram Soc 76:1985
14. Sun ZM, Zhou YC, Zhou J (2000) Phil Mag Lett 80:289
15. Thornton PH, Davies RG, Johnson TL (1970) Metal Trans1:207
16. Takeuchi S, Kuramoto E (1973) Acta Metall 21:415
17. Takeuchi S, Kuramoto E (1974) Acta Metall 22:429
18. Lall C, Chin S, Pope DP (1979) Metal Trans A 10:1323
19. Zhou YC, Sun ZM (to be published) J Europ.Ceram Soc
20. Barsoum M, El-Raghy T (1999) Metall Mater Trans A 30:363
21. Zhou Y, Sun Z (1999) Mater Res Innovat 2:360
22. Berkovitch-Yellin Z (1985) J Am Chem Soc 107:8239
23. Donnay JDH, Harker D (1937) Am Mineralogist 22:446
24. Low I (1998) J Europ Ceram Soc 18:709
25. Zhou YC, Sun ZM, Yu BH (2000) Z Metallkd 91:937
26. Gumbsch P, Riedle J, Hartmaier A, Fischmeister HF, (1998) Science 282:1293
27. Kear BH, Wildorf HGF (1962) Trans AIME 224:382